

# **Multiple-Coincidence Active Neutron Interrogation of Fissionable Materials**

**Tinsley, J.R., Hurley, J.P., and Trainham, R.**

**National Security Technologies, LLC/Special Technologies Lab, Santa Barbara, California**

**Keegan, R.P.**

**National Security Technologies, LLC/Remote Sensing Lab, North Las Vegas, Nevada**

## **Abstract**

In an extension of the Associated Particle Imaging technique that is used for the detection and imaging of hidden explosives, the present measurements use a beam of tagged 14.1 MeV neutrons in coincidence with two or more gammas to probe for the presence of fissionable materials. We have measured neutron-gamma-gamma coincidences with targets of depleted uranium, tungsten, lead, iron, and carbon and will present results that show the multiple-coincidence counting rate for the depleted uranium is substantially higher than any of the non-fissionable materials. In addition, the presence of coincidences involving delayed particle spectra provides a signature for fissionable materials that is distinct from that for non-fissionable ones. Information from the tagged neutron involved in the coincidence event is used to compute the position of the fissionable material in all three dimensions. The result is an imaging probe for fissionable materials that is compact and portable, and produces relatively low levels of background radiation. Simultaneous measurements on packages of interest for both explosives and fissionable materials are now feasible.

Key Words: Active interrogation, fissile materials, neutrons

## **Introduction**

Associated Particle Imaging is an active neutron interrogation technique that some of us have been developing at Special Technologies Laboratory (STL) for a number of years (Beyerle, 1990). By simultaneously identifying the position (in 3 dimensions) and elemental composition of materials, a substance of interest (such as a conventional explosive) can be located and identified even though it may be hidden in a closed container or a clutter of innocuous substances. Recently, we realized that this technique can easily be extended to the detection and location of fissile materials as well.

Although portal monitors that use passive radiation detection are in use in many areas, they are of limited effectiveness. Highly enriched Uranium (HEU) has a low rate of spontaneous fission, and the energies of the emitted  $\gamma$ -rays are so low as to be easily shielded. Weapons grade plutonium (WGPu) has a higher rate of spontaneous fission, but its radiation signature can also be muffled with sufficient shielding.

Active Neutron Interrogation (ANI) can address these issues and has other advantages as well. The flux of 14.1 MeV neutrons used to probe objects of interest is more penetrating than even high energy x-rays and induces the emission of radiation that can be detected, especially in the case of HEU. Since the conventional material detection technique can operate simultaneously with the fissile material detection, any object with substantial shielding material can be flagged as suspicious even in the absence of a fissile material detection. Finally, there is the possibility of detecting the presence of conventional explosives adjacent to the fissile material—the highest level of threat.

### **Theory of Operation**

ANI employs a small deuterium-tritium neutron generator which produces coincident neutrons and alpha particles, emitted in opposite directions (Fig. 1). A position-sensitive detector mounted on one side of the generator detects alphas, thus giving the time and direction of the corresponding neutron emission. When one of these “tagged” neutrons interacts with the material in its path, it frequently produces a  $\gamma$ -ray whose energy is characteristic of that material. An array of  $\gamma$  detectors (whose positions are known) measures the energy and arrival time of these  $\gamma$ -rays (relative to the neutron emission). The arrival time of the  $\gamma$ -ray is used to compute the distance traveled by the neutron along the known trajectory, so that the position of the interaction is known in all three dimensions. By recording many of these interactions, the distribution of material and its composition are determined.

Because the  $\gamma$ -rays are emitted from the nucleus uniformly in all directions, the  $\gamma$ -ray detectors may be put wherever is most convenient relative to the object under interrogation; specifically, they may be set on the same side of the object as the generator. This is an advantage over transmission x-ray

shadowgraphy, where the user must have access to both sides of the object. The number of detectors is limited only by cost (and possibly size and weight restrictions). Thus, it can be seen that the apparatus can be configured in any number of ways to meet differing goals.

The maximum useful neutron flux produced by the generator is in the range of  $3\text{--}5 \times 10^7$  n/s. The dose to personnel at these rates is generally below the recommended dose limits defined in ICRP-60 (ICRP, 1990). The relatively low radiation exposure confers an advantage over other active interrogation systems that generate much higher levels of radiation in the pursuit of their goals.

For the identification of conventional non-fissile substances, a single  $\gamma$ -ray is detected in coincidence with the outgoing neutron. This represents, most probably, an inelastic interaction between the neutron and a nucleus. The energy spectrum of these  $\gamma$ -rays is determined by the makeup of the material under interrogation. For example, explosives are identified by analyzing the C:N:O ratios found by comparing an unknown spectrum with the known spectra of these elements. The relative ratios of these three elements vary somewhat from one explosive to the next, but are significantly different from non-explosives.

In the case of fissile materials, the neutron interaction often induces fission, with the immediate emission of several  $\gamma$ -rays and several neutrons, followed by additional delayed  $\gamma$ -rays and neutrons (Verbinski, 1973; Sund, 1974). For these interactions, we require two or more  $\gamma$ -rays to be in coincidence with the neutron to distinguish them from inelastic scattering. The fission  $\gamma$ -rays have mostly a broad distribution centered near 1MeV; this distribution is quite similar for the various fissile elements, but different from those of non-fissile elements. The different trigger logic allows us to separate the two types of events so that they can be acquired simultaneously, but analyzed using different algorithms.

### **Experimental Details**

The geometry used to acquire the data presented here is shown in Fig. 2. A position-sensitive microchannel plate (MCP) detects the alpha particles incident on a window that is coated with a scintillator on the inside surface, resulting in a cone of tagged neutrons that has a half angle of

approximately  $7^\circ$ . Two 4" x 4" NaI(Tl) detectors were set forward and to the side of the tagged neutron beam. Each was shielded from the neutron generator by a 20-cm thickness of lead. Additional lead (not shown in the drawing) was put between the two detectors (but outside the cone of tagged neutrons) to greatly reduce the number of direct interactions between them.

### Measurements and Discussion

Due to the difficulty of obtaining kilogram quantities of HEU or WGPu, we used a 1.27-cm-thick plate of depleted uranium (DU) to test the fissile material response of the system. Results from a measurement with the plate set 60 cm from the neutron source are shown in Figs. 3 and 4. The time between neutron emission and particle detection in detector 1 is plotted against that for detector 2. The large peak corresponds to prompt n- $\gamma$ - $\gamma$  coincidences; the horizontal and vertical "arms" that extend from the peak correspond to delayed neutrons and  $\gamma$ -ray events in one detector in coincidence with a prompt  $\gamma$ -ray in the other.

The presence of a "bump" in the distribution of delayed events appears to be due to prompt neutrons that, traveling less than the speed of light and having a distribution of energies, reach the detectors later than the  $\gamma$ -rays. To test this speculation, additional measurements were made with the DU plate at 50 cm and 75 cm from the neutron source. The results are summarized in Fig. 5, which shows a 1D projection along one arm gated on the time corresponding to the arrival of prompt  $\gamma$ -rays in the other detector. The curves represent a Loess smoothing (Cleveland, 1977) to the data shown to guide the eye. The peaks corresponding to prompt events vary in time in accordance with the 50:60:75 ratio of time that the 14.1 MeV neutrons take to reach the DU plate (at  $5.13 \text{ cm ns}^{-1}$ ). The times between the peaks and the maxima of the delayed events follow reasonably closely to the 33:41.5:55 ratio of distance from the plate to the detectors. The breadth of the distribution also widens with distance, as expected. This leads us to conclude that a large fraction of the delayed events are due to neutrons.

Note that most of the events that correspond to the DU are in the prompt  $\gamma$ -ray peak, with equal event times (to within the system resolution). This gives us the distance to the target, which in

conjunction with the known trajectory of the neutron gives us its location in three dimensions. Thus, we retain the same 3D imaging capability with fissile material detection that we have enjoyed with non-fissile material detection.

Next, measurements were made using several non-fissile elements — lead, tungsten, iron, and carbon — to demonstrate the difference between their response and that of the DU. The three metals were in the form of 1.27-cm-thick plates, so that the volume intercepted by the neutron beam was constant; the carbon target was a cube, approximately 10 cm on each side. For each of these measurements, plots of the coincidence times for the two detectors are shown in Figs. 6–9. As with Fig. 3, the color scale in each plot has been normalized to the highest channel so that the full range of data values can be seen. Thus, the (random) background in the DU plot is very faint relative to the strong coincident peak, and in carbon, with its minimal coincidence response, the background is quite prominent.

The strength of the coincident peak in lead and tungsten is just 10% of that in DU (normalized to integrated beam dose) and close to 40% in iron; the carbon response is minimal. Note that the delayed particle “arms” seen in the DU spectrum are not so prominent in these other elements. Even in the absence of any delayed particle emission from these elements, we expect a faint signal in this region due to the probability of seeing a random n- $\gamma$  coincidence in one detector paired with a prompt  $\gamma$ -ray coincidence in the other.

The relatively high response in iron can be attributed to its relatively large cross section for interaction with 14.1 MeV neutrons and the fact that the dominant reaction involves a cascade that produces simultaneous 847 keV and 1238 keV  $\gamma$ -rays. Since iron is so common, it may be necessary to use other information to aid in distinguishing the two. In the other extreme, carbon is essentially invisible due to the fact that it emits only one  $\gamma$ -ray, at 4439 keV. The minimal number of counts over background seen at the location where a peak is found for the other elements is probably due to interactions with the target support structure. A similar response is seen in “empty” target measurements.

An illustration of the delayed response versus the prompt response for iron, lead, and carbon is compared with that for DU in Fig. 10. Again, a 1D projection along one arm is gated on the time corresponding to the arrival of prompt gammas in the other detector. Each trace is normalized to the same neutron dose. Clearly, DU has a uniquely strong delayed response with structure that is not seen in the other spectra.

## Conclusions

The data collected this year indicate that this technique gives a unique signature of fission. We also conclude that both prompt  $\gamma$ -ray and neutron pulses are observed in our data. Fissionable material could be distinguished based upon the  $\gamma$ -ray “spike” alone; however, the observation of a neutron “spike” displaced by the neutron flight time is a definitive indicator of fission. Furthermore, the fission cross section for HEU and WGPu in response to 14.1 MeV neutrons is twice that for DU.

Sufficient information can be collected to simultaneously detect, image, and identify both explosives and fissionable material. The ability to perform these functions using a neutron interrogation system that presents no health physics issues is very significant and unique. The experimental work this year has demonstrated the viability of the concept. Further physics work is needed to determine the response to the presence of shielding, masking material, and generator-interrogated-object distance.

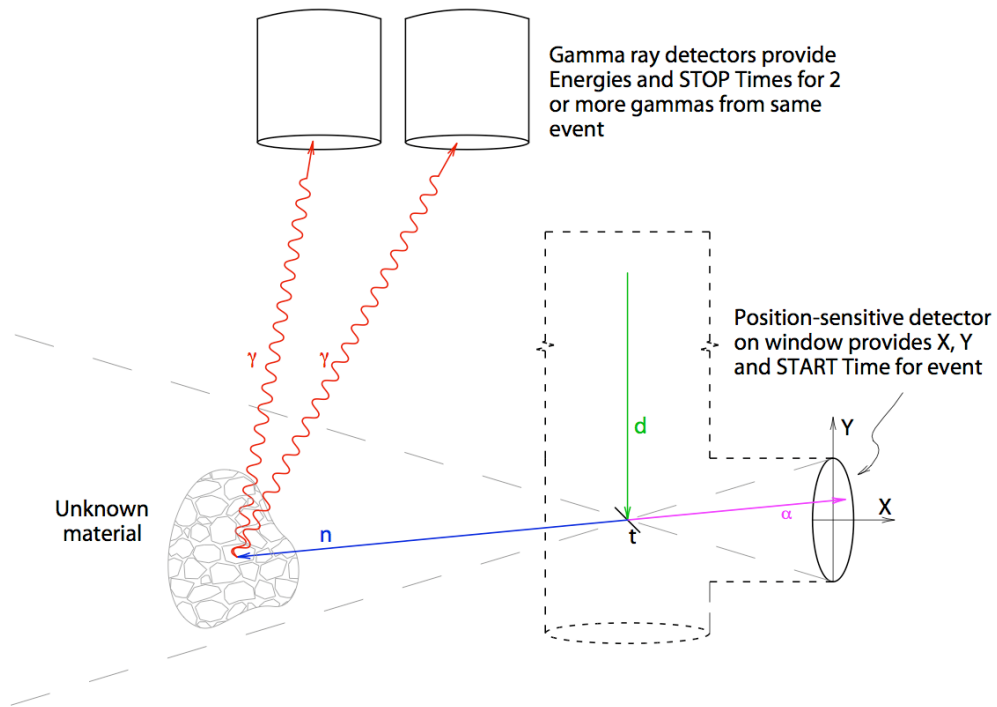
## References

- Beyerle, A, Hurley, J P, and Tunnell, L, Design of an associated particle imaging system. Nuclear Instruments and Methods in Physics Research, A, vol. 299: 458–462; 1990.
- Cleveland, WS, Robust locally weighted regression and smoothing scatterplots. J. Am. Stat. Assoc. 74: 829–836; 1977.
- Sund, RE, Weber, H, and Verbinski, VV, Isomeric gamma rays from  $^{235}\text{U}(n,f)$  and  $^{239}\text{Pu}(n,f)$  for times less than 1  $\mu\text{sec}$  after fission. Phys. Rev. C, 10: 853–870; 1974. Available at: [http://prola.aps.org/abstract/PRC/v10/i2/p853\\_1](http://prola.aps.org/abstract/PRC/v10/i2/p853_1).

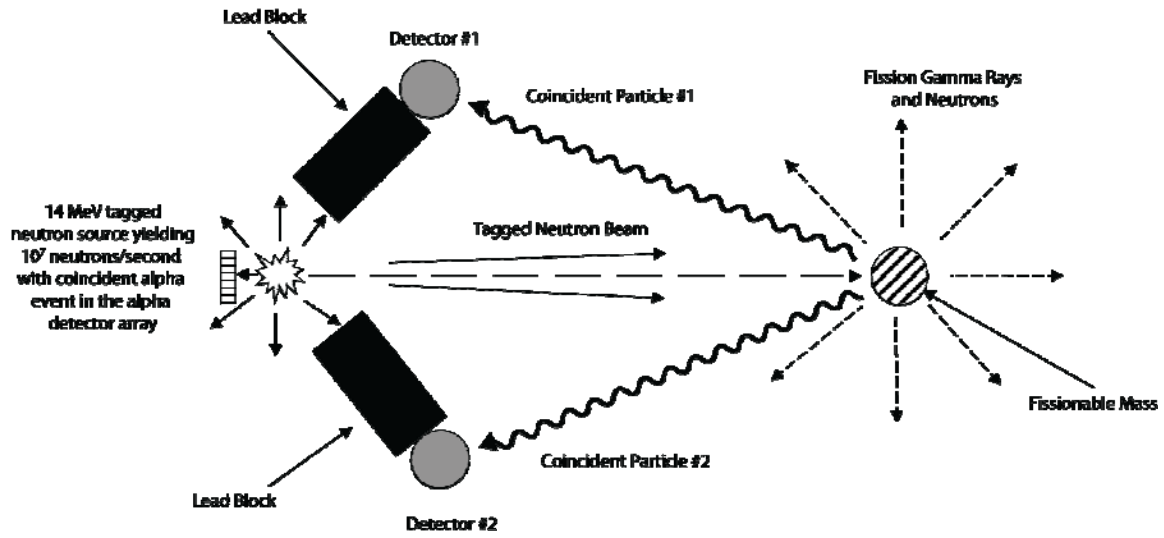
Verbinski, VV, Weber, H, and Sund, RE, Prompt Gamma Rays from  $^{235}\text{U}(n,f)$ ,  $^{239}\text{Pu}(n,f)$ , and Spontaneous Fission of  $^{252}\text{Cf}$ . Phys. Rev. C, 7: 1173–1185; 1973. Available at [http://prola.aps.org/abstract/PRC/v7/i3/p1173\\_1](http://prola.aps.org/abstract/PRC/v7/i3/p1173_1).

ICRP-60, 1990 Recommendations of the International Commission on Radiological Protection, Volume 21, Nos. 1–3, 1991.

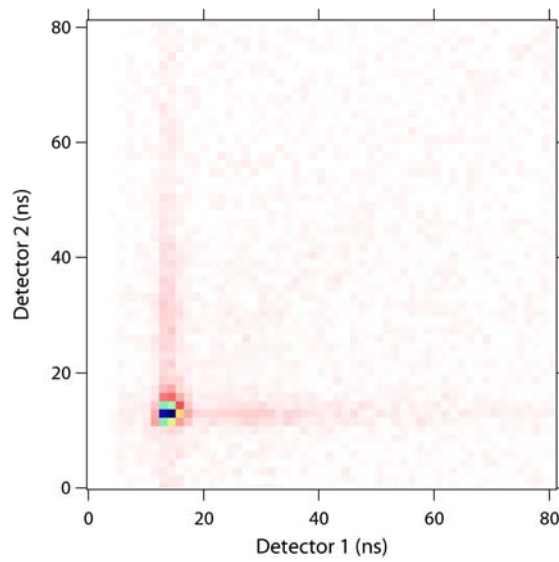
**Fig. 1** How ANI is used to identify materials



**Fig. 2** Fissile material detection using active neutron interrogation

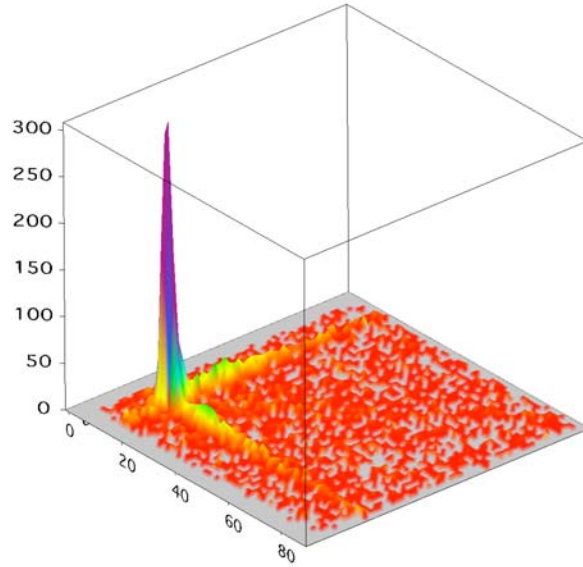


**Fig. 3** Two dimensional view of data from a DU plate set 60 cm from the neutron source

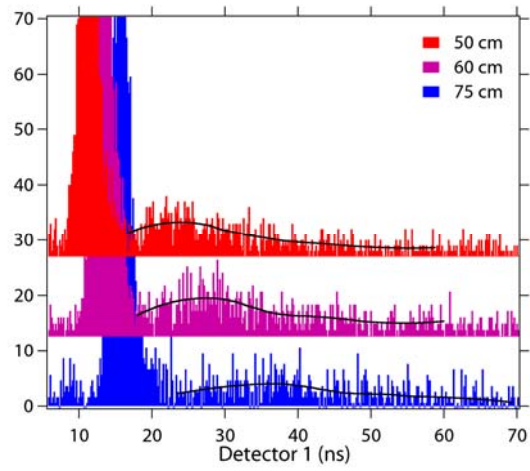


**Fig. 4** Three dimensional view of data from a DU plate set 60 cm from the neutron source

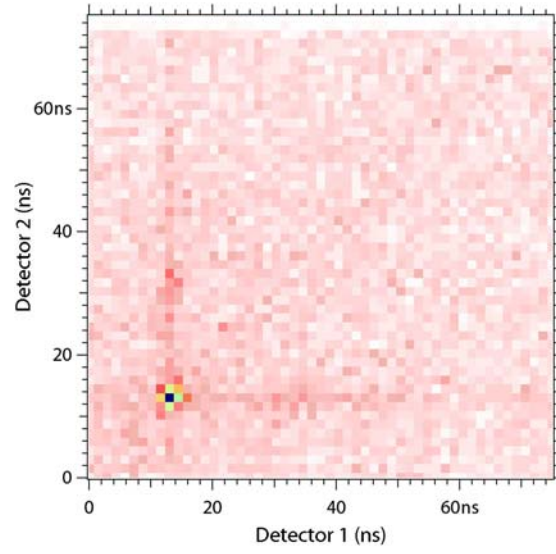




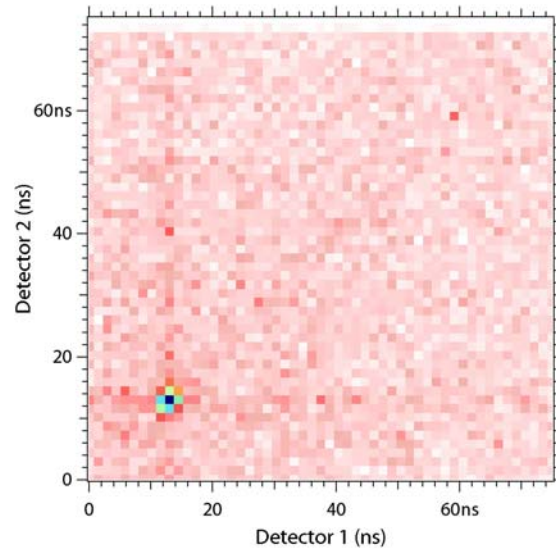
**Fig. 5** Detail along one “arm” for DU at several distances from the neutron source



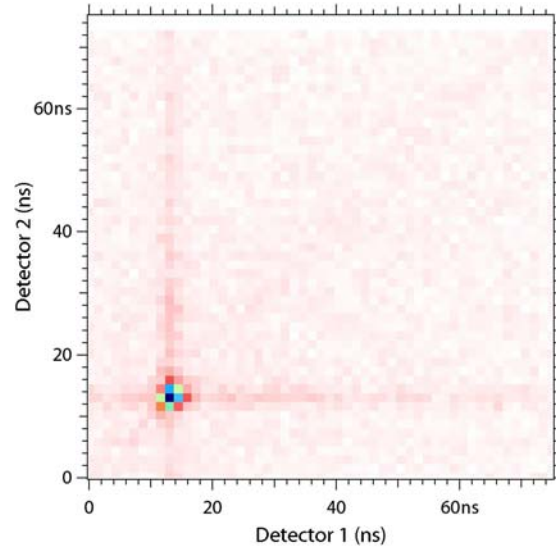
**Fig. 6** Lead



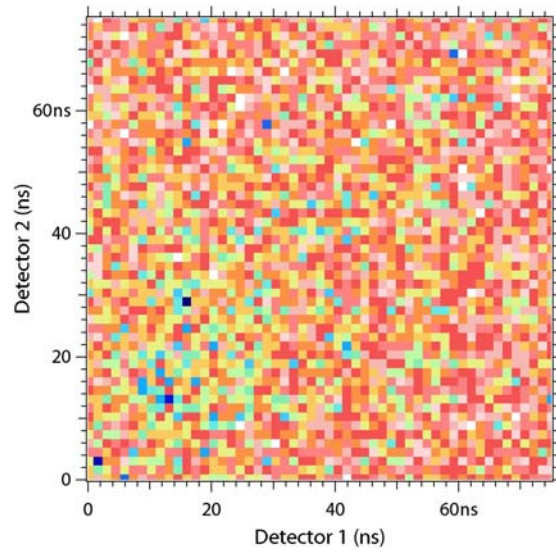
**Fig. 7** Tungsten



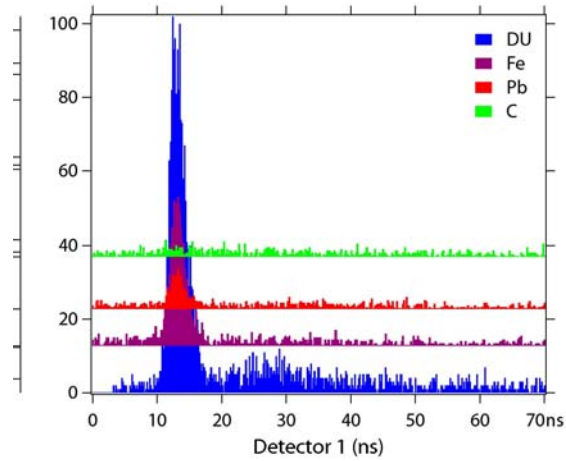
**Fig. 8** Iron



**Fig. 9** Carbon



**Fig. 10** Detail along one “arm” for DU, iron, lead, and carbon



This manuscript has been authored by National Security Technologies, LLC, under Contract No. DE-AC52-06NA25946 with the U.S. Department of Energy. The United States Government retains and the publisher, by accepting the article for publication, acknowledges that the United States Government retains a non-exclusive, paid-up, irrevocable, world-wide license to publish or reproduce the published form of this manuscript, or allow others to do so, for United States Government purposes.